Activity-Dependent Neurite Outgrowth: Implications for Network Development and Neuronal Morphology

6

Arjen van Ooyen, Jaap van Pelt, Michael A. Corner, and Stanley B. Kater

Empirical studies have shown that high levels of neuronal activity can cause neurites to retract, whereas lower levels allow further outgrowth. Using simulation studies, we have explored the possible implications of such activity-dependent neurite outgrowth for network development and neuronal morphology. These implications include a transient phase of high connectivity during development, the presence of multiple stable end states of development at different connectivity levels, and the emergence of size differences between the neuritic fields of excitatory and inhibitory cells. These phenomena, which are also observed in developing cultures of cerebral cortex cells, emerge in the model without assuming predetermined, time-scheduled mechanisms.

6.1 Introduction

Electrical activity, in the form of action potentials and synaptically driven fluctuations in membrane potential, plays an important role in the development of neurons into functional neural networks. This activity-dependent maturation begins even before the onset of sensory responses, and is driven by intrinsically generated patterns of electrical discharges. Most studies, theoretical as well as empirical, have largely focused on activity-dependent changes in synaptic strength, but many other processes that determine network connectivity and neuronal function are, on a variety of time scales, also modulated by electrical activity. These include naturally occurring cell death (see chapter 9), neurite outgrowth and branching, synaptogenesis, elimination of synapses, changes in the number and effectiveness of ion channels and neurotransmitter receptors (see chapter 8), and even gene expression (for reviews, see Van Ooyen, 1994; Corner et al., 2002).

As a result of these activity-dependent processes, a reciprocal influence exists between the development of neuronal form, function, and connectivity on the one hand (''slow dynamics''; different time scales are involved, but they are all slow relative to the time scale of the dynamics of electrical activity) and neuronal and network activity on the other hand (''fast dynamics''). Thus, the activity patterns generated by a developing network can modify the organization of the network and the functional characteristics of the neurons, leading to altered activity patterns, which in turn can further modify structural and functional characteristics.

Electrical activity exerts its effects on multiple time scales (hours, e.g., number and effectiveness of neurotransmitter receptors; days or weeks, e.g., neurite outgrowth and synapse formation) as well as on multiple levels of organization [individual synapses, e.g., long-term potentiation (LTP) and depression (LTD); whole cell, e.g., neuronal excitability and neurite outgrowth; population of cells, e.g., balance of excitation and inhibition]. In many cases, the way in which activity modifies network connectivity and neuronal function contributes to the homeostasis of neuronal activity (for reviews, see Van Ooyen, 1994; Turrigiano, 1999; Abbott and Nelson, 2000; Corner et al., 2002). When the activity of a neuron is high, neuronal connectivity and excitability are modified

by activity-dependent processes such as neurite outgrowth (see section 6.2), changes in ionic conductances (Turrigiano et al., 1994, 1995) and neurotransmitter receptors (Turrigiano et al., 1998; see also chapter 8), and changes in the balance of excitation and inhibition (Corner and Ramakers, 1992; Turrigiano, 1999) so as to decrease activity. When the activity of a neuron is low, on the other hand, neuronal connectivity and excitability will be modified so as to increase activity.

In this chapter we focus on activity-dependent neurite outgrowth and explore its implications for network development and neuronal form. Section 6.2 describes the empirical studies, which have established that high levels of neuronal activity often cause neurites to retract (mediated by changes in intracellular calcium levels), whereas lower levels allow further outgrowth. Section 6.3 briefly reviews modeling studies of activity-dependent neurite outgrowth and some other activity-dependent processes. In section 6.4 we describe in detail a model of activity-dependent neurite outgrowth.

6.2 Activity-Dependent Neurite Outgrowth—Neurobiological Background

Neurite elongation, branching, and steering are under the control of the growth cone, a specialized structure at the tip of a growing neurite (Letourneau et al., 1991). Growth cones consist of a central zone containing organelles and microtubules (long polymers of tubulin that form a continuous core within the neurite) and surrounded by spikelike protrusions (filopodia) and fan-shaped sheets (lamellipodia), both of which are filled with actin filaments. Polymerization of tubulin into microtubules—which for the most part takes place at the growth cone—provides the driving force for neurite elongation. The actin cytoskeleton mainly serves to control branching and steering (Acebes and Ferrús, 2000), but also participates in elongation. The tension generated by the rearward flow of fibrillar actin (F-actin) in the growth cone slows down elongation, probably by affecting the rate of microtubule polymerization (Buxbaum and Heidemann, 1992; Lin and Forscher, 1995).

Neurite outgrowth is sensitive to the calcium concentration within the growth cone, $[Ca^{2+}]_{in}$. Calcium affects the polymerization and depolymerization of microtubules, both directly (e.g., Schilstra et al., 1991) and via its influence on microtubule-associated proteins (MAPs). By interacting with microtubules, MAPs regulate many aspects of microtubule dynamics, not only polymerization and depolymerization, but also bundling, spacing, and interactions with actin filaments (Maccioni and Cambiazo, 1995). Calcium modulates MAP function by regulating the phosphorylation state of MAPs (Sánchez et al., 2000).

The dynamics of the actin cytoskeleton are also influenced by calcium. The (de)polymerization of F-actin and the formation of cross-linked meshworks and bundles of actin filaments are controlled by actin-binding proteins, many of which are modulated by calcium (Forscher, 1989). The Rho proteins are particularly important for growth cone morphology and neurite branching (Aspenstrom, 1999; Cline, 1999; Li et al., 2000). These are involved in the organization of the actin cytoskeleton and are essential for the formation of lamellipodia and filopodia (Tapon and Hall, 1997; Aspenstrom, 1999; see also chapters 3 and 4). Rho proteins, too, may be modulated by calcium (Ramakers et al., 1998; Chen et al., 1998).

Because of the strong dependence of neurite outgrowth on calcium, any factor that can change $[Ca^{2+}]_{in}$—such as depolarization, neurotransmitters (Cohan et al., 1987; Berridge, 1998), neurotrophins

(Stoop and Poo, 1996), and cell adhesion molecules (Bixby et al., 1994), which affect calcium influx through voltage- and ligand-gated calcium channels —will be able to affect neurite outgrowth (for reviews, see Goldberg and Grabham, 1999; McAllister, 2000).

Large increases in $[Ca^{2+}]_{in}$—caused, for example, by high levels of neuronal electrical activity (action potentials) or by depolarization induced by neurotransmitters or depolarizing media—arrest neurite outgrowth and can even cause retraction (e.g., Cohan and Kater, 1986; Fields et al., 1990; Mattson and Kater, 1989; Mattson et al., 1988; Torreano and Cohan, 1997). Growth cones can generate transient elevations of $[Ca^{2+}]_{in}$ as they migrate (Gomez and Spitzer, 1999), and, consistent with the results mentioned earlier, the rate of axon elongation is inversely proportional to the frequency of these spontaneous calcium transients (Gu and Spitzer, 1995; Gomez and Spitzer, 1999). However, decreases in $[Ca^{2+}]_{in}$ (e.g., as a result of lowered neuronal electrical activity) can also suppress neurite elongation (e.g., Mattson and Kater, 1987; Mattson, 1988; Lankford and Letourneau, 1991; Al-Mohanna et al., 1992; Ramakers et al., 2001), while in some cases neurite elongation can be promoted by elevations of $[Ca^{2+}]_{in}$ above the resting level (e.g., Kuhn et al., 1998).

These seemingly contradictory results are accommodated by Kater's calcium hypothesis for neurite outgrowth, which states that deviations in either direction from an optimal $[Ca^{2+}]_{in}$ slow down neurite elongation (Kater et al., 1988; Kater and Mills, 1991). Deviations within the physiological range are already effective, so that calcium signaling in the growth cone is indeed physiologically relevant (reviewed in Goldberg and Grabham, 1999).

The bell-shaped dependence of neurite elongation on $[Ca^{2+}]_{in}$ implies that one cannot predict a priori whether a given change in $[Ca^{2+}]_{in}$ has a growth-promoting or growth-inhibiting effect (Kater and Mills, 1991). This will depend on the magnitude of the change as well as on the existing resting calcium levels. Moreover, the optimal $[Ca^{2+}]_{in}$ for outgrowth may be different for different neurons (Kater et al., 1988; Kater and Mills, 1991). Furthermore, it is worthwhile to distinguish between the effects of calcium on the morphology of the growth cone (number and extent of its protrusions—filopodia and lamellipodia) and the effects of calcium on neurite elongation. For example, focal increases in $[Ca^{2+}]_{in}$ can induce the formation of protrusions (Davenport and Kater, 1992), which may slow the forward movement of the growth cone, and thus neurite elongation, through lateral interactions with the environment (Goldberg and Grabham, 1999).

In addition to affecting neurite elongation, calcium levels and depolarization influence neurite branching (Schilling et al., 1991; Sanes and Takács, 1993; Ramakers et al., 1998, 2001). Both increased and reduced branching have been observed following depolarization (for reviews, see Cline, 1999; Acebes and Ferrús, 2000; McAllister, 2000). So, as for elongation, there may be an optimal calcium level for branching, which could be different for different cell types.

The stimuli that change $[Ca^{2+}]_{in}$ in the growth cone can act on the level of a single neurite or on the level of the whole cell. For example, local application of glutamate to a single dendrite results in regression of that dendrite (Mattson et al., 1988), whereas somatic action potentials may simultaneously regulate the behavior of all the growth cones and neurites of a given neuron (Cohan and Kater, 1986; Kater and Guthrie, 1990), for example, by propagation of action potentials into the dendrites (Stuart and Sakmann, 1994) or by other mechanisms (electrotonic spread, calcium dynamics).

6.3 Review of Models

Hentschel and Fine (1996) used Kater's calcium hypothesis for neurite outgrowth to study the emergence of dendritic forms from initially spherical cells (see chapter 3). In their model, local outgrowth of the cell membrane is taken to depend on the local concentration of calcium close to the internal surface of the membrane.

Whereas Hentschel and Fine (1996) used Kater's hypothesis to study the development of dendritic forms in single, isolated cells, we used Kater's hypothesis to study the development of synaptically connected networks from initially unconnected cells (see section 6.4).

Abbott and Jensen (1997) studied calcium-dependent neurite outgrowth in combination with calcium-regulated conductances (see chapter 8). As in our model, they used the concept of a circular neuritic field to model outgrowth and connectivity, but instead of modeling firing frequency (see section 6.4.1), they used spiking neurons and also explicitly modeled the dynamics of intracellular calcium. Starting from random initial conditions, the model cells develop spontaneously into a coupled network displaying a complex pattern of activity. Although the cells are governed by identical equations, they differentiate within these networks and show a wide variety of intrinsic characteristics.

Raijmakers and Molenaar (1999) applied activity-dependent neurite outgrowth to the maturation of connections in an ART (adaptive resonance theory) neural network model of memory, and Eglen et al. (2000) studied the role of neurite outgrowth in the formation of retinal mosaics (see chapter 7).

Activity-dependent neurite outgrowth contributes to the homeostasis of neuronal activity (see section 6.1). Other forms of homeostatic plasticity include mechanisms for regulating the intrinsic excitability of neurons (ionic conductances, neurotransmitter receptors; for a review, see Corner et al., 2002) and mechanisms for stabilizing total synaptic strength (Turrigiano, 1999). Modeling studies have begun to explore the implications of these forms of plasticity for network development and function (e.g., LeMasson et al., 1993; Marder et al., 1996; Horn et al., 1998; Golowasch et al., 1999; see also chapter 8). In contrast to Hebbian mechanisms, where changes in synaptic strength occur in a synapse-specific manner, homeostatic plasticity acts on the neuronal level. Neurite outgrowth, too, operates on a higher level than that of a single synapse. A change in a cell's axonal or dendritic extent means that the connectivity with many other cells is changed simultaneously. During development, homeostatic plasticity ensures that neurons remain responsive to their inputs and allows Hebbian plasticity to modify synaptic strengths selectively (Turrigiano, 1999). During aging, homeostatic plasticity can account for maintenance of memory systems that undergo synaptic turnover and degradation (Horn et al., 1998).

6.4 Detailed Description of a Model of Activity-Dependent Neurite Outgrowth

The goal of the model that we present in this section (see Van Ooyen and Van Pelt, 1994; Van Ooyen et al., 1995) is not to reproduce any particular system in detail, but rather to explore the range of phenomena that could result from activity-dependent neurite outgrowth. In the model, the growth of both excitatory and inhibitory neurons is activity dependent, and all the cells are initially unconnected. Development into a connected network (slow dynamics) takes place

only under the influence of the activity (fast dynamics) that is generated by the network itself (no external input). Growing neurons are modeled as expanding neuritic fields, and neurons become connected when their neuritic fields overlap. The outgrowth of each neuron depends upon its own level of electrical activity, according to Kater's theory for the control of neurite outgrowth (thus we do not model calcium explicitly, assuming that $[Ca^{2+}]_{in}$ is proportional to the level of neuronal electrical activity). The dependence of outgrowth on activity in an individual neuron is such that when activity is higher than a critical value, its neuritic fields retract (reducing its connectivity with other cells and thus, in general, its activity), and when it is lower, its neuritic fields expand (increasing its connectivity and activity). Thus, by adapting the size of its neuritic field, a neuron attempts to maintain a certain level of activity (homeostasis), the aforementioned critical value, at which the neuron's neuritic field remains stationary.

The model is inspired in part by cultures of dissociated cerebral cortex cells (e.g., Van Huizen et al., 1985; for a review, see Marom and Shahaf, 2002), whose development into a network (without external input) by neurite outgrowth and synaptogenesis shows many similarities with that in vivo. The phases through which the cultured networks pass during development—with respect to electrical activity and connectivity—as well the effects of various treatments, such as chronically blocking activity, have been described extensively (see section 6.4.4). In section 6.4.4, the phenomena observed in the model are compared with those observed in culture.

6.4.1 Neuron Model

The shunting model (Grossberg, 1988), transformed into dimensionless equations, is used to describe neuronal activity. In this model, excitatory inputs drive the membrane potential toward a maximum (the excitatory saturation potential), while inhibitory inputs drive the membrane potential toward a minimum (the inhibitory saturation potential):

$$\frac{dX_i}{dT} = -X_i + (1 - X_i)\sum_{k=1}^{N} W_{ik}F(X_k) - (H + X_i)\sum_{l=1}^{M} W_{il}F(Y_l) \tag{6.1}$$

$$\frac{dY_j}{dT} = -Y_j + (1 - Y_j)\sum_{k=1}^{N} W_{jk}F(X_k) - (H + Y_j)\sum_{l=1}^{M} W_{jl}F(Y_l), \tag{6.2}$$

where X_i and Y_j are the membrane potentials of, respectively, the excitatory cell i and the inhibitory cell j, expressed in units of excitatory saturation potential; N and M are the total number of excitatory and inhibitory cells, respectively; H is the ratio of inhibitory to excitatory saturation potential; T is time expressed in units of membrane time constant; the Ws denote the connection strengths (all $W \geq 0$; k and l are the indices of the excitatory and inhibitory driver cells, respectively; i and j are the indices of the excitatory and inhibitory target cells, respectively); and $F(X)$ is the mean firing rate, which is taken to be a sigmoidal function of the membrane potential:

$$F(X) = \frac{1}{1 + e^{(\theta - X)/\alpha}}, \tag{6.3}$$

where α determines the steepness of the function and θ represents the firing threshold. The low firing rate when the membrane potential is subthreshold represents spontaneous activity.

6.4.2 Outgrowth and Connectivity

Neurons are randomly placed on a two-dimensional surface. Each neuron is given a circular "neuritic field," the radius of which is variable. When two such fields overlap, both neurons become connected with a strength proportional to the area of overlap:

$$W_{ij} = A_{ij}S, \tag{6.4}$$

where $A_{ij} = A_{ji}$ is the amount of overlap, representing the total number of synapses formed reciprocally between neurons i and j ($A_{ii} = 0$); and S is a constant of proportionality, representing the average synaptic strength. Strength may depend on the type of connection. We distinguish S^{ee}, S^{ei}, S^{ie}, and S^{ii}, where, for example, S^{ei} is the inhibitory-to-excitatory synaptic strength.

In this abstraction, no distinction has been made between axons and dendrites, so the connections among excitatory cells and among inhibitory cells are symmetrical. The main findings of the model do not change, however, if separate axonal and dendritic fields are implemented (see the section on differences among cells and section 6.5).

In the model, the outgrowth of each neuron, whether excitatory or inhibitory, depends in an identical way upon electrical activity:

$$\frac{dR_i}{dT} = \rho G[F(X_i)], \tag{6.5}$$

where R_i is the radius of the neuritic field of neuron i, $F(X_i)$ is the firing frequency of neuron i, and ρ determines the rate of outgrowth. The outgrowth function G is defined as

$$G[F(X_i)] = 1 - \frac{2}{1 + e^{[\varepsilon - F(X_i)]/\beta}}, \tag{6.6}$$

where ε is the value of $F(X_i)$ for which $G = 0$, and β determines the steepness of the function. Depending on $F(X_i)$, a neuritic field will grow out [$G > 0$ when $F(X_i) < \varepsilon$], retract [$G < 0$ when $F(X_i) > \varepsilon$], or remain constant [$G = 0$ when $F(X_i) = \varepsilon$] (see figure 6.1A). All cells will thus attempt to get a neuritic field size for which the input from overlapping cells is such that $F(X_i) = \varepsilon$; in other words, ε is a "homeostatic setpoint." Equation (6.6) is a phenomenological description of the theory of Kater et al. (see section 6.2). It is not a complete bell-shaped curve, but the precise rates of outgrowth are not essential for the results as long as with high activity, neuritic fields retract and with low activity, they expand. What could produce new results is if a growth function is used for which cells also retract when neuronal activity is below a certain level (figure 6.1B). However, using such a function yields similar results, provided that the initial activity is high enough (see the section on an alternative growth function).

6.4.3 Parameters

The fraction of inhibitory cells, $M/(N + M)$, is taken in the range of 0.1–0.2 (e.g., Meinecke and Peters, 1987). For the rest, all the parameter values are the same for excitatory and inhibitory cells. The outgrowth of neurons is on a time scale of days or weeks (Van Huizen et al., 1985; Schilling et al., 1991), so connectivity is quasi-stationary on the time scale of membrane potential dynamics. To avoid unnecessarily slowing down the simulations, ρ is chosen as large as possible under the quasi-stationary approximation. In most simulations, we use $\rho = 0.0001$. As nominal values for the other parameters, we chose $H = 0.1$, $\theta = 0.5$, $\alpha = 0.1$, $\beta = 0.1$, and $\varepsilon = 0.6$.

6.4.4 Results of the Model

In most of the following subsections, the results of the model are given first, followed by the empirical

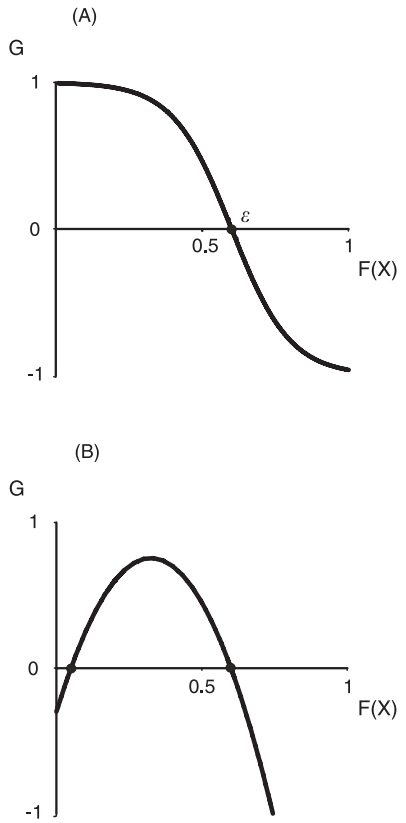

Figure 6.1
Growth functions relating the rate of neurite outgrowth (G) with firing rate [$F(X)$]. (A) The growth function [see Eq. (6.6)] as used in most of the simulations. The neuritic field of a neuron retracts when the neuronal firing rate is above ε. (B) A growth function for which the neuritic field of a neuron also retracts when the firing rate falls below some critical value.

data from cultures of dissociated cells that can be accounted for by the model.

Overshoot in Excitatory Networks

Model

Simulation shows that one of the implications of activity-dependent outgrowth, together with a hysteresis relationship between network connectivity and activity (see the following discussion), is that a developing network goes through a phase in which the connectivity, or number of synapses, is considerably higher than in the final, stable situation; i.e., the network exhibits overshoot in connectivity (figure 6.2A). For a purely excitatory network ($M = 0$), this result can be predicted directly from Eq. (6.1). For a given connectivity matrix $\mathbf{W}$, the equilibrium points are solutions of

$$0 = -X_i + (1 - X_i) \sum_{k=1}^{N} W_{ik} F(X_k) \qquad \forall i. \tag{6.7}$$

If all cells have the same ε and the variations in X_i are small relative to $\overline{X}$, the average membrane potential of the network, we find (Van Ooyen and Van Pelt, 1994):

$$0 \cong -\overline{X} + (1 - \overline{X})\, \overline{W} F(\overline{X}), \tag{6.8}$$

where $\overline{W}$ is the average connection strength. Based on this approximation,

$$\overline{W} = \frac{\overline{X}}{(1 - \overline{X}) F(\overline{X})} \qquad 0 \leq \overline{X} < 1. \tag{6.9}$$

Thus, this equation, which defines a manifold (plotted in figure 6.2B), gives the equilibrium value(s) of $\overline{X}$ for a given value of $\overline{W}$. Equilibrium states on branch CD of the manifold are unstable with respect to $\overline{X}$; equilibrium states on the other branches are stable. Because changes in $\overline{W}$—arising from

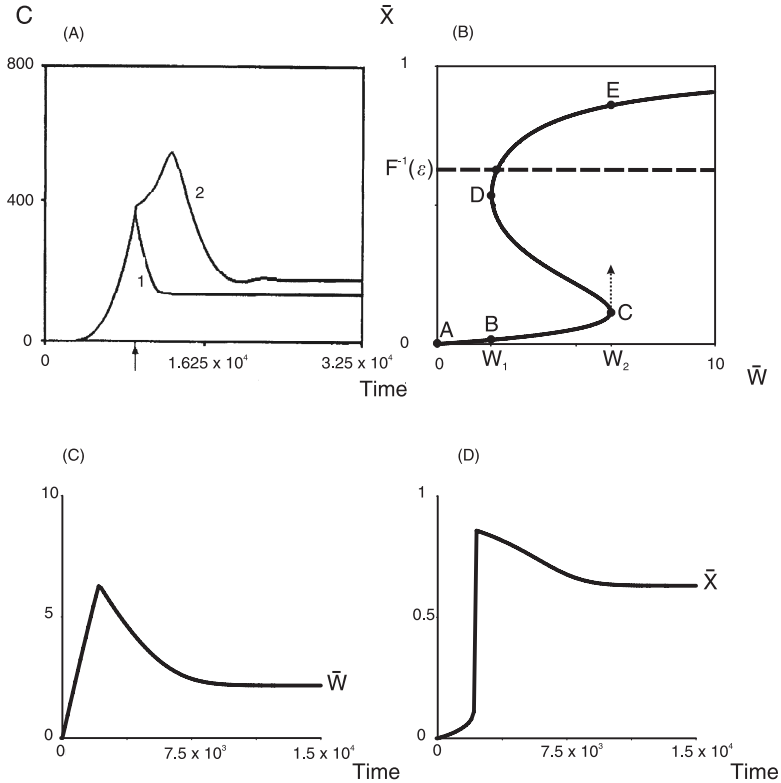

Figure 6.2
Overshoot in connectivity during development. (*A*) Total connectivity $C = \sum_{p=1,q=1}^{N+M} A_{pq}$ in (1) a network without inhibition and (2) a network with inhibition. The arrow indicates the onset of network activity in the network with inhibition. (From Van Ooyen et al., 1995.) (*B*) Hysteresis relationship between average membrane potential $\overline{X} = (1/N)\sum_{i=1}^{N} X_i$ at steady state for a given value of $\overline{W}$, and average connection strength $\overline{W} = (1/N)\sum_{i=1,k=1}^{N} W_{ik}$ in a purely excitatory network [see Eq. (6.9)]. The intersection point with the line $\overline{X} = F^{-1}(\varepsilon)$ is the equilibrium point of the system, at which $\overline{W}$ remains constant. (From Van Ooyen and Val Pelt, 1994.) See section 6.4.4. (*C*) To arrive at the equilibrium point in (*B*), a developing network, starting at point *A* in (*B*), has to go through a phase in which $\overline{W}$ is higher than in equilibrium. (*D*) The average membrane potential during development.

outgrowth and retraction of neuritic fields—are very much slower than changes in $\overline{X}$, $\overline{W}$ can be considered as quasi-stationary on the time scale of the membrane potential dynamics. In other words, in the time that $\overline{X}$ relaxes to its equilibrium value (for a given $\overline{W}$), $\overline{W}$ hardly changes. The slow evolution of $\overline{X}$, determined by changes in $\overline{W}$, therefore takes place along the equilibrium manifold defined by Eq. (6.9); this manifold is sometimes referred to as the slow manifold.

At the intersection point with the line $\overline{X} = F^{-1}(\varepsilon)$ (F^{-1} is the inverse of F), $\overline{W}$ remains constant; above and below that line, it decreases and increases, respectively [see Eq. (6.6)]. Consider the case in which the intersection point is on the branch DE (figure 6.2B). In a developing network, connectivity and activity are initially low, and $\overline{W}$ increases; $\overline{X}$ follows the branch ABC until it reaches W_2, at which point $\overline{X}$ jumps to the upper branch, thus exhibiting a transition from a quiescent to an activated state. But the activity in the network is then so high that the neuritic fields begin to retract and $\overline{W}$ to decrease, and so $\overline{X}$ moves along the upper branch from E to the intersection point. Thus, in order to arrive at an equilibrium point on the branch DE, a developing network has to go through a phase in which the average connectivity is higher than in the final situation. In other words, a higher connectivity is needed to trigger activity in a quiescent network than to sustain it once the network has been activated (hysteresis). The existence of such hysteresis (i.e., the S-shaped curve of figure 6.2B) hinges upon the firing rate function F having a firing threshold and low but nonzero values for subthreshold membrane potentials.

Empirical

A general feature of nervous system development, in vivo and in vitro, is that many structural elements show an initial overproduction followed by an elimination during further development. These so-called

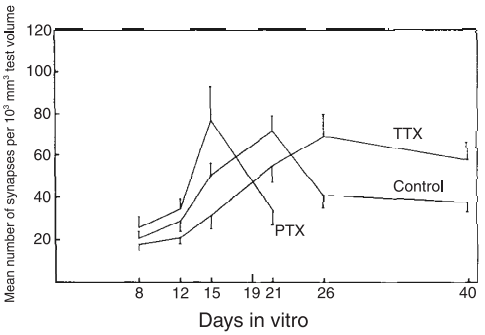

Figure 6.3
Cultures of dissociated cerebral cortex cells show a transient overproduction of synapse numbers (Control). Chronic blockade of activity (by tetrodotoxin, TTX) largely prevents synapse elimination, whereas intensification of activity (by picrotoxin, PTX, which blocks inhibition) accelerates the process. (After Van Huizen et al., 1985, 1987a.)

overshoot phenomena occur, for example, with respect to total dendritic length (Uylings et al., 1990), number of dendrites and axons (e.g., Gorgels et al., 1989), and synapse numbers (e.g., O'Kusky, 1985). The mechanism underlying the generation of overshoot in the model may provide part of the explanation for overshoot phenomena, at least for those that have been observed in vitro. For example, cultures of dissociated cerebral cortex cells show a transient overproduction of synapses during development (Van Huizen et al., 1985, 1987a), with a phase of neurite outgrowth and synapse formation during the first 3 weeks in vitro being followed by a substantial elimination of synapses during the week thereafter (figure 6.3). The development of electrical activity in these cultures also shows a good correspondence with the model. With increasing synaptic density, single-neuron firing and network activity abruptly appear within a window of a few days (Habets et al., 1987). Electrical activity appears to control both neurite outgrowth and synapse elimination. Chronic blockade of

electrical activity enhances neurite outgrowth (Van Huizen and Romijn, 1987) and prevents subsequent synapse elimination (Van Huizen et al., 1985). Developing cerebellar cultures have also been shown to exhibit a sequence of events similar to that in the model (Schilling et al., 1991).

Periodic Behavior in Excitatory Networks

Model

The level of electrical activity (or $[Ca^{2+}]_{in}$) above which neurites retract may be different for different classes of neurons (Guthrie et al., 1988; Kater et al., 1988). In terms of the model, this means that there can be variation among cells in ε, the level of electrical activity above which the neuritic field retracts. Under these conditions, complex periodic behavior can occur, with individual cells displaying oscillations that differ in frequency and amplitude (figure 6.4C,D) (Van Ooyen and Van Pelt, 1996). The precise behavior depends on the spatial distribution of the cells and the distribution of ε values over the cells. Note that the oscillations in activity are caused by retraction and outgrowth of the cells' neuritic fields and thus occur on a time scale of days. The network as a whole still shows overshoot in connectivity, but instead of going to a stable connectivity level, the network connectivity (and activity) keeps oscillating to some degree.

Empirical

Using a multielectrode setup to record activity patterns in developing cultures of dissociated cortex cells, Van Pelt et al. (2003) have observed fluctuations in the level of electrical activity of individual cells, with periods of increased activity sometimes lasting as long as several days. Whether these are correlated with periodic changes in neurite outgrowth and connectivity, as the model suggests, is now being investigated.

Overshoot in Mixed Networks

Model

We now consider networks that contain both excitatory and inhibitory cells. Simulation shows that overshoot still takes place in the presence of inhibition, and can even be enhanced (figure 6.2A). To counterbalance inhibition, a higher excitatory connectivity is necessary to reach the level of electrical activity at which the average connectivity starts declining.

Whereas in purely excitatory networks the decline in connectivity begins shortly after the onset of network activity, in mixed networks the decline in overall connectivity can be considerably delayed relative to the onset of network activity (figure 6.2A). In parts of the network with many inhibitory cells, excitatory cells can still be growing out, while in parts with fewer inhibitory cells they are already retracting. For the overshoot curve this implies that average connectivity can still increase markedly after the onset of network activity. Blocking inhibition will thus advance the process of overshoot.

Empirical observations show that the development of inhibition tends to lag behind that of excitation (reviewed in Corner et al., 2002). Modeling the delayed development of inhibition by giving the inhibitory cells a lower outgrowth rate results in a less pronounced excitatory overshoot and a growth curve of the number of inhibitory connections that no longer exhibits any overshoot. The inhibitory cells develop into a network that is already approaching a more or less stable level of electrical activity, and will therefore simply grow out until their overlap is such that $F(X_i) = \varepsilon$.

Empirical

The observation in the model that the decline in connectivity can occur earlier in purely excitatory networks than in mixed networks (figure 6.2A) is

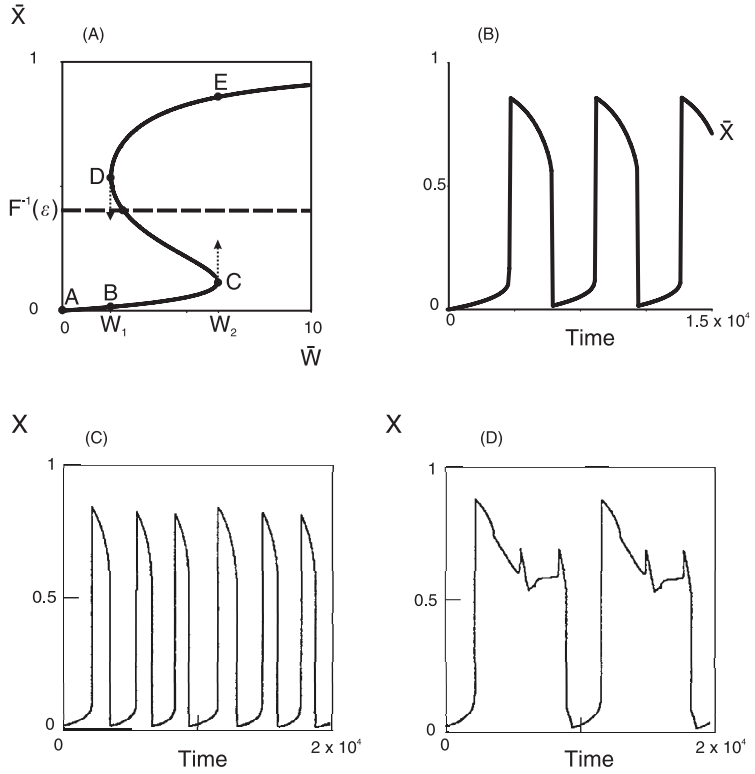

Figure 6.4
Oscillations in electrical activity as a result of periodic changes in neurite outgrowth. (*A*) See also figure 6.2B. If the value of ε is such that the intersection point of the line $\overline{X} = F^{-1}(\varepsilon)$ and the hysteresis curve is on the branch *CD*, regular oscillations occur, in both average connectivity and average membrane potential, that follow the path *ABCEDBCED*. . . . The period of these oscillations is determined by the value of ρ [see Eq. (6.5)]. (*B*) The oscillations in the average membrane potential. (*C*, *D*) If the value of ε is not approximately equal for all cells in the network [so that the approximation on which (*A*) is based cannot be made], complex periodic behavior can occur. Here are shown the oscillations in membrane potential for two different cells in a network in which there is variation in ε values. The cell in (*C*) has $\varepsilon = 0.15$; the cell in (*D*) has $\varepsilon = 0.68$. (From Van Ooyen and Van Pelt, 1996.)

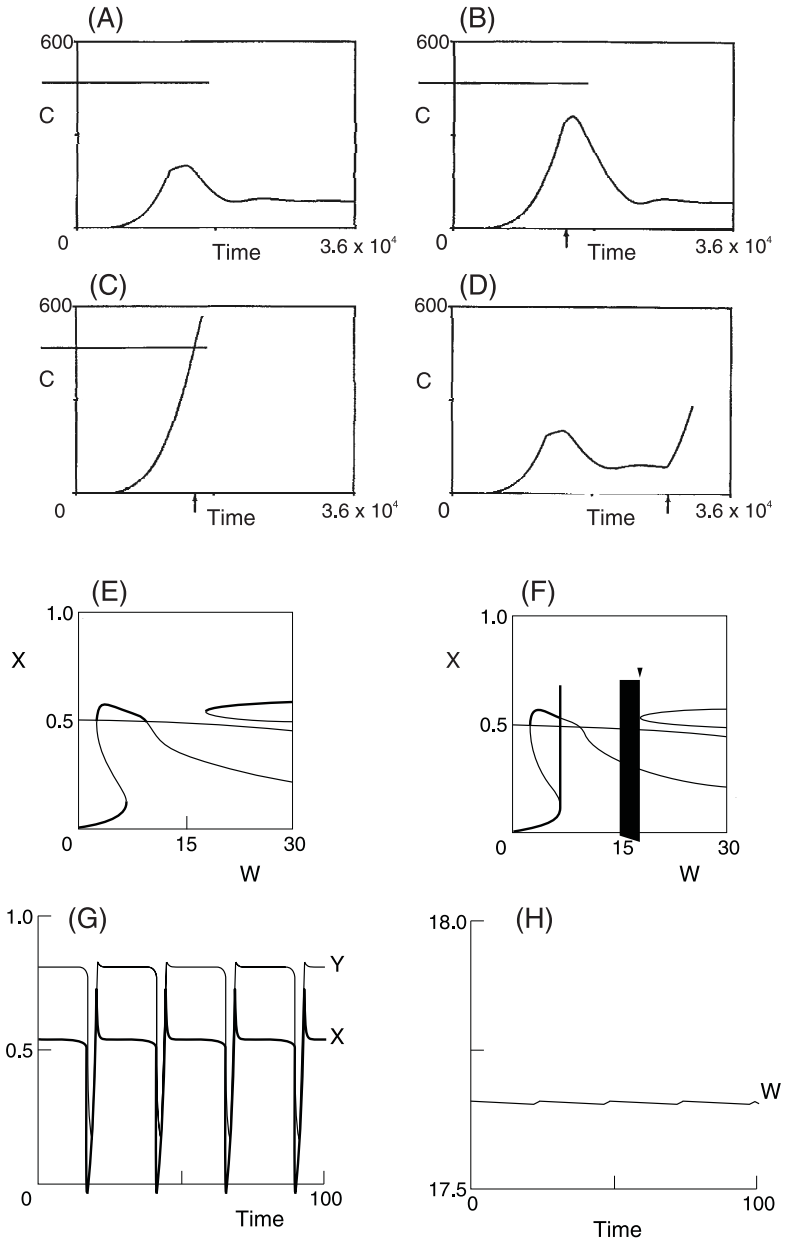

Figure 6.5
If the connection strength in a network with excitatory and inhibitory cells is larger than a critical value, connectivity will not be reduced to the normal equilibrium value. (*A*) Normal development in a mixed network. C = total connectivity =

in agreement with the observation in culture that chronic blockade of GABAergic (i.e., γ-aminobutyric acid) transmission advances the process of synapse elimination (Van Huizen et al., 1987a) (figure 6.3). The presence of inhibition can account for the observation in culture that the decline in connectivity is delayed relative to the onset of network activity (Van Huizen et al., 1985).

Delayed development of inhibition, which in the model causes the number of inhibitory connections to fail to exhibit overshoot, offers a putative explanation for the observation in culture that the synapses on dendritic shafts (presumably inhibitory; Shepherd, 1990) show no overshoot during development, whereas the synapses on dendritic spines, which are mostly excitatory, account for the overshoot phenomenon (Van Huizen et al., 1985).

Multistability, Critical Period, and Periodic Behavior in Mixed Networks

Model

Under all initial conditions, purely excitatory networks go to the same global end state with respect to electrical activity and average connection strength. Mixed networks, however, do not necessarily do so. In a network with a moderate level of inhibition and an initial average connection strength (of both excitatory and inhibitory connections) that is larger than a critical value, connectivity will not be reduced to the normal equilibrium value but instead will continue to increase (figure 6.5C; Van Ooyen et al., 1995). Basically, this is because the increased inhibitory connection strength stimulates further outgrowth. Van Oss and Van Ooyen (1997) studied this effect in a simplified model consisting of one excitatory and one inhibitory unit. These units can be interpreted as single cells or as representing populations of cells. The excitatory unit (with membrane potential X) is connected to itself and to the inhibitory unit, while the inhibitory unit (with membrane potential Y) is connected only to the excitatory unit and not to itself. Furthermore, it is assumed that the connection between the excitatory and the inhibitory unit is symmetrical (this assumption is not essential for the results) and that the connection strength between the excitatory and the inhibitory unit is a fraction p of the connection strength W of the excitatory unit to itself. The latter assumption is reasonable because when a cell's neuritic field increases, its connection strength with both

$\sum_{p=1,\,q=1}^{N+M} A_{pq}$. (*B, C*) Electrical activity is blocked until the time indicated by the arrow. In this period, connectivity can only increase. If the level of connectivity thus reached is higher than the level indicated by the horizontal line, connectivity is not reduced, but continues to increase when activity is allowed to return. (*D*) Activity is blocked in a normally developed network at the time indicated by the arrow. (*E*) The slow manifold of X, where both $dX/dT = 0$ and $dY/dT = 0$, and the W-nullcline (the thin, nearly horizontal line), where $dW/dT = 0$, in the simplified model (see the section on multistability in mixed networks). The bold lines indicate stable equilibrium points with respect to X and Y (when W is regarded as a parameter), and the thin lines indicate the unstable ones. The intersections of the manifold and the W-nullcline are the equilibrium points of the system. (*F*) The slow manifold (without showing stability) and the W-nullcline. The bold lines are trajectories: one, starting at $W = 0$ and $X = 0$, approaches the normal point attractor at low W; the other one, starting at $W = 15$ and $X = 0$, approaches the limit cycle attractor at high W (see arrow). Starting at $W = 15$, X and Y oscillate while W slowly increases until the oscillations "touch" the fold of the slow manifold, at which point there is no further net increase in W. Note that since the changes in W are much slower than in X and Y, no separate oscillations are visible. (*G*) Time plot of the limit cycle attractor in (*F*) showing X (bold line) and Y. (*H*) Time plot of the limit cycle attractor in (*F*) showing W. (From Van Ooyen et al., 1995, and Van Oss and Van Ooyen, 1997.)

excitatory and inhibitory cells increases. The simplified model in differential equations is

$$\frac{dX}{dT} = -X + (1 - X)WF(X) - (H + X)pWF(Y) \tag{6.10}$$

$$\frac{dY}{dT} = -Y + (1 - Y)pWF(X) \tag{6.11}$$

$$\frac{dW}{dT} = q(\varepsilon - bW^2 - X), \tag{6.12}$$

where H is the inhibitory saturation potential and q determines the rate at which the connection strength increases. Because the rate of neurite outgrowth [ρ in Eq. (6.5)]—and thus the rate at which the connection strength changes—is low compared with the dynamics of the membrane potential, q is small. Compared with Eq. (6.6), the growth function [Eq. (6.12)] is simplified to $(\varepsilon - X)$, which has the same qualitative behavior as Eq. (6.6). To prevent connectivity from increasing indefinitely, a saturation term $-bW^2$ is added, where b is small. Without this term, however, the model gives essentially the same results. The model is simple enough to be studied by bifurcation analysis and elaborate enough to show the same phenomena as in the full network model [Eqs. (6.1), (6.2), and (6.5)].

Bifurcation analysis shows that in most cases there is a point attractor (attractor A) at a low connectivity level and a limit cycle attractor at a high connectivity level (attractor B) (figure 6.5E,F). Attractor B is interpretable as a ''pathological'' state; the limit cycle has fast, epileptiform oscillations in electrical activity (figure 6.5G). Under the normal initial conditions for a developing network (namely, a low level of connectivity), the system develops normally and ends up, via an overshoot in connectivity, in attractor A, whereas a high initial connectivity will cause the system to end up in attractor B (a high initial connectivity can be brought about by, for example, blocking electrical activity for a certain time during network formation). Furthermore, the model shows that the higher the level of inhibition during development (e.g., number of inhibitory cells, strength of inhibitory synapses), the more likely the system is to end up in attractor B.

Empirical

The presence of two stable attractors at different connectivity levels can explain the observation in culture that following chronic blockade of electrical activity (thus causing enhanced neurite outgrowth and a high density of synapses, i.e., a high level of connectivity), there is no subsequent elimination of the excess synapses when the block is finally removed and activity returns to control levels (Van Huizen et al., 1987b, Van Huizen and Romijn, 1987).

In the model, the higher the level of inhibition during development, the more likely the system is to end up in pathological attractor B with strong oscillatory activity (epileptiform activity). This is in line with the following observation: Hypoxic-ischemic encephalopathy (HIE, i.e., brain damage as result of lack of oxygen) induced in rat pups can lead to permanent epileptiform activity later on in adulthood (Romijn et al., 1994), but this epileptiform activity is not the result of a preferential loss of inhibitory elements such as GABAergic nerve endings; indeed, there is a preferential survival of inhibitory elements in the damaged areas (Romijn et al., 1993).

Differences among Cells and Differentiation between Excitatory and Inhibitory Cells

Model

The neuritic field size adapts to the local cell density, resulting in small fields in dense areas and larger ones in sparse areas. Cell death in a mature network will

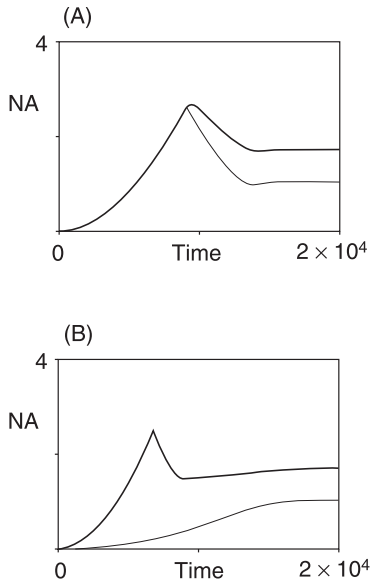

Figure 6.6
The average neuritic field area (NA) of excitatory cells (thick lines) becomes smaller than that of inhibitory cells (thin lines). The network has torus boundary conditions. In (*A*), the inhibitory cells have the same outgrowth rate as the excitatory cells; in (*B*), the inhibitory cells have a lower outgrowth rate than the excitatory cells. (From Van Ooyen et al., 1995.)

result in a compensatory increase in the neuritic fields of the surviving neurons. After excitatory cell loss, electrical activity decreases, and cells will begin to grow out until they all have the same activity level as before [$F(X_i) = \varepsilon$]. To compensate for the lost cells, a larger neuritic field is necessary.

Although in the model there are no intrinsic differences in growth properties between excitatory and inhibitory cells, their neuritic fields will nevertheless become different. The neuritic fields of inhibitory cells tend to become smaller than those of excitatory cells (figures 6.6 and 6.7), and the mechanism accounting for this is as follows: Each cell will attain a neuritic field size for which the input from overlapping cells is such that $F(X_i) = \varepsilon$. An excitatory cell that receives inhibition therefore needs more excitatory input than a cell that is not inhibited, and thus grows a larger neuritic field. As a consequence, each inhibitory cell will become surrounded by large, strongly connected excitatory cells, whereas, since the same growth rules apply to inhibitory cells, the inhibitory cell itself can remain small because a small neuritic field yields sufficient overlap with its large surrounding cells. In other words, an inhibitory cell becomes small by increasing the size of its direct neighbors. These neighbors, in turn, will become surrounded by relatively small cells, and so on (figure 6.7).

When separate axonal and dendritic fields are used in the model, differentiation between excitatory and inhibitory cells still occurs (the other results are also robust to modeling axonal and dendritic fields separately; see section 6.5). Let R_i^{d} be the radius of the dendritic field of cell i, and R_i^{a} that of its axonal field. As a dendritic field receives input from axonal fields, Eq. (6.4) becomes

$$\begin{aligned} W_{ij} &= O(R_i^{\mathrm{d}}, R_j^{\mathrm{a}})S \\ W_{ji} &= O(R_j^{\mathrm{d}}, R_i^{\mathrm{a}})S, \end{aligned} \tag{6.13}$$

where $O(\ )$ gives the area of overlap and S represents synaptic strength. The growth of both types of fields is governed by Eq. (6.6) in which, in order to have axonal fields larger than dendritic fields, the growth rate of the latter is given a smaller value ($\rho^{\mathrm{d}} < \rho^{\mathrm{a}}$). With this procedure, inhibitory cells still become smaller than excitatory cells. Even if the axonal field of an inhibitory cell is kept at a constant size, its dendritic field becomes smaller than the fields of the excitatory cells. Excitatory cells receiving input via the (constant) axonal field of a neighboring inhibitory cell will get large dendritic and axonal fields, so that the dendritic

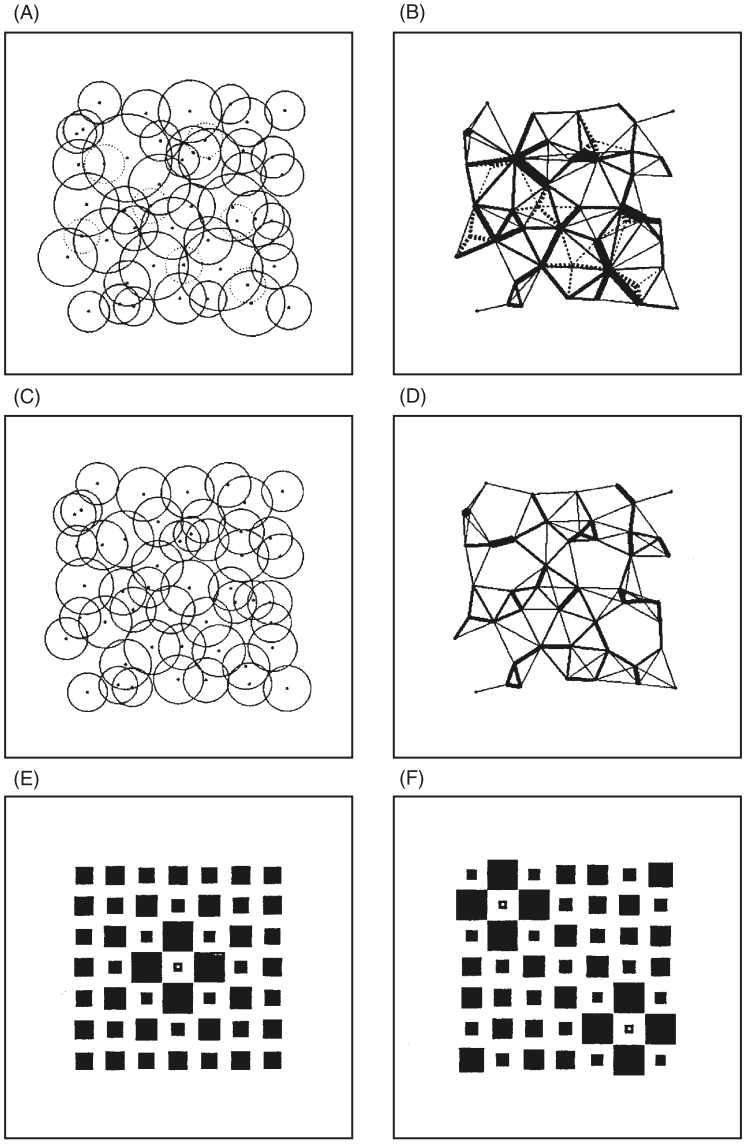

Figure 6.7
Patterns of neuritic field sizes imposed by inhibitory cells. All networks have torus boundary conditions. (*A*) Mature network with excitatory and inhibitory cells. A dotted line indicates an inhibitory cell. (*B*) Graph showing the connections in the network of (*A*). The line width is proportional to the connection strength. A dashed line indicates a connection between an inhibitory and an excitatory cell. Connections that cross boundaries are not shown. (*C*) Same placing of cells as in (*A*), but all former inhibitory cells are now excitatory. (*D*) Graph showing connections in network of (*C*). (*E*) Cells on grid positions. The diameter of a square is proportional to the area of the neuritic field. Scaled to maximum area. The cell with a white dot in the middle is inhibitory. (*F*) Same as in (*E*), but with two inhibitory cells. (From Van Ooyen et al., 1995.)

field of the inhibitory cell can remain small to get sufficient input.

Empirical

The model shows that excitatory cell loss will be accompanied by an increased neuritic (dendritic) field of the surviving neurons. In the human cortex, the dendritic extent per neuron increases steadily through old age (Coleman and Flood, 1986), which has been interpreted as a compensatory response to neuronal death (Coleman and Flood, 1986). This is consistent with the model and with the observation that no increase in dendritic extent occurs in brain regions that do not lose neurons with age (Coleman et al., 1986).

In the model, the neuritic fields of inhibitory cells tend to become smaller than those of excitatory cells. In the cerebral cortex, the dendritic (and axonal) fields of inhibitory neurons are indeed smaller, on the whole, than those of excitatory neurons. Pyramidal cells, which are excitatory, have large apical dendrites (which often cross several layers) and long axons. The nonpyramidal cells, most of which are inhibitory, usually have dendritic and axonal branches that extend only locally (e.g., Abeles, 1991).

Alternative Growth Function

In the growth function [Eq. (6.6)] used in the model, neurite retraction takes place only when neuronal activity is too high. If a growth function is used in which neurite retraction can also take place when neuronal activity is too low (see figure 6.1B), all the main results still hold, provided that the initial activity (as a result of initial connectivity and/or spontaneous activity) is high enough to stimulate outgrowth (Van Ooyen et al., 1996). A difference with this growth function is that not all cells will necessarily become part of the network; cells that receive too little excitation from their surrounding cells will completely retract their neuritic fields.

6.5 Discussion

It has previously been realized that activity-dependent neurite outgrowth could have considerable potential for controlling neuronal form and circuitry (e.g., Mattson, 1988). The model studies described in this chapter have begun to make this potential explicit. The way in which activity influences neurite outgrowth contributes to the homeostasis of neuronal activity, and our model studies have shown that this striving for homeostasis may underlie many of the seemingly unrelated phenomena observed in developing cultures of dissociated neurons. The phenomena that may be the consequence of activity-dependent neurite outgrowth, and that are observed both in culture and in the model, include (1) a transient phase of high connectivity during development, (2) the presence of stable end states of development at different connectivity levels, and (3) size differences in neurite length between excitatory and inhibitory cells. Without modeling studies, it would have been impossible to surmise that these three effects could be different aspects of the same underlying process.

With respect to effect (2), the model has shown that the state of the network (e.g., the average connectivity level) and the balance between excitatory and inhibitory elements can determine whether normal development will take place. Thus, *too much* inhibition prevents the normal pruning of exuberant connections and results in a network with highly oscillatory electrical activity (epileptiform activity).

With respect to effect (3), one must not draw the conclusion that intrinsic differences are unimportant in the development of size differences, but some aspects of differentiation can take place without them.

The results of the model do not depend critically on the neuritic fields being described as circles. Other

approaches for modeling neurite outgrowth and connectivity give essentially the same results as described here (Van Ooyen and Van Pelt, 1994). Also, modeling axonal and dendritic fields separately, so that connectivity is no longer necessarily symmetrical, does not alter the main findings (see the section on alternative growth function and Van Ooyen et al., 1995).

Activity-dependent neurite outgrowth could play a role not only during development but also in the adult nervous system. Many studies have shown structural changes in axons and dendrites in response to lesions, aberrant activity, changes in environmental conditions, and behavioral training (for a review, see Woolley, 1999).

Future Modeling Studies

Our modeling studies have dealt with the implications of activity-dependent neurite outgrowth for neuronal morphology and gross network development. Possible roles of activity-dependent neurite outgrowth in learning and memory have not been studied (but see Raijmakers and Molenaar, 1999; see also section 6.3). A form of memory could occur when, after the application of external input, the network is pushed into a different stationary state with respect to neuritic field sizes and connectivity.

A first step toward a more detailed description of growing neurons will be to use, instead of circular neuritic fields, spatial functions describing the density of the neuron's axonal and dendritic branches. Connectivity between neurons can then be described as a convolution of the overlapping dendritic and axonal spatial density functions.

A second step toward a more detailed description could be to model the growing neurites themselves (for example, using a compartmental modeling approach; see chapter 4). The outgrowth of each neurite can then be made dependent on the (time-averaged) local membrane potential at the tip of the neurite (the growth cone). This membrane potential will be influenced by both the firing rate at the soma and the local synaptic potentials at the neurite. In this approach, the effects of neuronal activity on neurite branching can also be incorporated.

Besides making the description of the growing neurites more detailed, the neuron model can be improved upon. Spiking neurons can be used, and the dynamics of intracellular calcium can be modeled explicitly (as in Abbott and Jensen, 1997). This has the advantages that outgrowth can be made directly dependent on intracellular calcium, the major mediator of activity-dependent neurite outgrowth (see section 6.2), and that the effects of different firing patterns on neurite outgrowth can be included. For example, Fields et al. (1990) found that phasic stimulation is more effective in inhibiting neurite outgrowth than stimulation with the same number of impulses at a constant frequency, an effect for which the calcium dynamics could be responsible.

Finally, activity-dependent neurite outgrowth can be studied in combination with other activity-dependent processes, such as changes in conductances of membrane currents (see chapter 8 and Abbott and Jensen, 1997).

Future Experimental Studies

Experiments are necessary for studying the extent to which activity-dependent neurite outgrowth indeed underlies the phenomena listed in section 6.4.4. Ideally, one would like to simultaneously record the morphological development and neuronal activity of individual cells in a developing network. Using a multielectrode setup, Van Pelt et al. (2003) can continuously record the electrical activity of up to sixty cells in a developing network for a period of at least 6 weeks in culture. In order to correlate activity history

with morphology, steps are being undertaken to determine the morphology of the cells from which activity has been recorded.

Examples of the many specific questions that can now be investigated include the following:

• Do neurites retract or change their morphology when they become electrically active?

• Does synaptic input from inhibitory cells indeed influence the size of the dendrites of excitatory cells?

• Do excitatory cells in purely excitatory networks have less variation in the size of their neuritic extent than excitatory cells in a mixed network (as the model predicts; compare figures 6.7A and 6.7C)?

• Does the failure of synapse elimination to occur after chronically blocking electrical activity depend upon the length of the blockade? The model predicts that as long as the blockade does not exceed a critical time, and the connectivity level is therefore below a critical value, elimination of surplus synapses will still occur.

• Do the slow fluctuations observed in the level of electrical activity of individual cells correlate with periodic changes in neurite outgrowth?

It would be useful for further modeling studies if the relationship between intracellular calcium concentration and rate of outgrowth could be determined more quantitatively.

References

Abbott, L. F., and Jensen, O. (1997). Self-organizing circuits of model neurons. In *Computational Neuroscience, Trends in Research*, J. Bower, ed. pp. 227–230. New York: Plenum.

Abbott, L. F., and Nelson, S. B. (2000). Synaptic plasticity: Taming the beast. *Nat. Neurosci.*, Suppl. 3: 1178–1183.

Abeles, M. (1991). *Corticonics. Neural Circuits of the Cerebral Cortex*. Cambridge: Cambridge University Press.

Acebes, A., and Ferrús, A. (2000). Cellular and molecular features of axon collaterals and dendrites. *Trends Neurosci.* 23: 557–565.

Al-Mohanna, F. A., Cave, J., and Bolsover, S. R. (1992). A narrow window of intracellular calcium concentration is optimal for neurite outgrowth in rat sensory neurones. *Dev. Brain Res.* 70: 287–290.

Aspenstrom, P. (1999). The Rho GTPases have multiple effects on the actin cytoskeleton. *Exp. Cell Res.* 246: 20–25.

Berridge, M. J. (1998). Neuronal calcium signaling. *Neuron* 21: 13–26.

Bixby, J. L., Grunwald, G. B., and Bookman, R. J. (1994). Ca^{2+} influx and neurite outgrowth in response to purified N-cadherin and laminin. *J. Cell Biol.* 127: 1461–1475.

Buxbaum, R. E., and Heidemann, S. R. (1992). An absolute rate theory model for tension control of axonal elongation. *J. Theor. Biol.* 155: 409–427.

Cline, H. T. (1999). Development of dendrites. In *Dendrites*, G. Stuart, N. Spruston, and M. Häusser, eds. pp. 35–67. Oxford: Oxford University Press.

Cohan, C. S., and Kater, S. B. (1986). Suppression of neurite elongation and growth cone motility by electrical activity. *Science* 232: 1638–1640.

Cohan, C. S., Connor, J. A., and Kater, S. B. (1987). Electrically and chemically mediated increases in intracellular calcium in neuronal growth cones. *J. Neurosci.* 17: 3588–3599.

Coleman, P. D., and Flood, D. G. (1986). Dendritic proliferation in the aging brain as a compensatory repair mechanism. *Prog. Brain Res.* 70: 227–237.

Coleman, P. D., Buell, S. J., Magagna, L., Flood, D. G., and Curcio, C. A. (1986). Stability of dendrites in cortical barrels of C57B1/6N mice between 4 and 45 months. *Neurobiol. Aging* 7: 101–105.

Corner, M. A., and Ramakers, G. J. A. (1992). Spontaneous firing as an epigenetic factor in brain development—physiological consequences of chronic tetrodotoxin and picrotoxin exposure on cultured rat neocortex neurons. *Dev. Brain Res.* 65: 57–74.

Corner, M. A., Van Pelt, J., Wolters, P. S., Baker, R. E., and Nuytinck, R. H. (2002). Effects of sustained blockade of

excitatory synaptic transmission on spontaneously active developing neuronal networks—an inquiry into the reciprocal linkage between intrinsic biorythms and neuroplasticity in early ontogeny. *Neurosci. Biobehav. Rev.* 26: 127–185.

Chen, H. J., Rojas, S. M., Oguni, A, and Kennedy, M. B. A. (1998). A synaptic Ras-GTPase activating protein (p135 SynCap) inhibited by CaM kinase II. *Neuron* 20: 895–904.

Davenport, R. W., and Kater, S. B. (1992). Local increases in intracellular calcium elicit local filopodial responses in *Helisoma* neuronal growth cones. *Neuron* 9: 405–416.

Eglen, S. J., Van Ooyen, A., and Willshaw, D. J. (2000). Lateral cell movement driven by dendritic interactions is sufficient to form retinal mosaics. *Network: Comput. Neural Syst.* 11: 103–118.

Fields, R. D., Neale, E. A., and Nelson, P. G. (1990). Effects of patterned electrical activity on neurite outgrowth from mouse sensory neurons. *J. Neurosci.* 10: 2950–2964.

Forscher, P. (1989). Calcium and polyphosphoinositide control of cytoskeletal dynamics. *Trends Neurosci.* 12: 468–474.

Golowasch, J., Casey, M., Abbott, L. F., and Marder, E. (1999). Network stability from activity-dependent regulation of neuronal conductances. *Neur. Comput.* 11: 1079–1096.

Goldberg, D. J., and Grabham, P. W. (1999). Braking news: Calcium in the growth cone. *Neuron* 22: 423–425.

Gomez, T. M., and Spitzer, N. C. (1999). *In vivo* regulation of axon extension and pathfinding by growth-cone calcium transients. *Nature* 397: 350–355.

Gorgels, T. G. M. F., De Kort, E. J. M., Van Aanholt, H. T. H., and Nieuwenhuys, R. (1989). A quantitative analysis of the development of the pyramidal tract in the cervical spine cord in the rat. *Anat. Embryol.* 179: 377–385.

Grossberg, S. (1988). Nonlinear neural networks: Principles, mechanisms, and architectures. *Neur. Net.* 1: 17–61.

Gu, X., and Spitzer, N. C. (1995). Distinct aspects of neuronal differentiation encoded by frequency of spontaneous Ca^{2+} transients. *Nature* 375: 784–787.

Guthrie, P. B., Mattson, M. P., Mills, L., and Kater, S. B. (1988). Calcium homeostasis in molluscan and mammalian neurons: Neuron-selective set-point of calcium rest concentrations. *Soc. Neurosci. Abstr.* 14: 582.

Habets, A. M. M. C., Van Dongen, A. M. J., Van Huizen, F., and Corner, M. A. (1987). Spontaneous neuronal firing patterns in fetal rat cortical networks during development in vitro: A quantitative analysis. *Exp. Brain Res.* 69: 43–52.

Hentschel, H. G. E., and Fine, A. (1996). Diffusion-regulated control of dendritic morphogenesis. *Proc. Roy. Soc. London B* 263: 1–8.

Horn, D., Levy, N., and Ruppin, E. (1998). Neuronal regulation versus synaptic unlearning in memory maintenance mechanisms. *Network: Comput. Neural Syst.* 9: 577–586.

Kater, S. B., and Guthrie, P. B. (1990). Neuronal growth cone as an integrator of complex environmental information. *Cold Spring Harbor Symp. Quant. Biol.* LV: 359–370.

Kater, S. B., and Mills, L. R. (1991). Regulation of growth cone behaviour by calcium. *J. Neurosci.* 11: 891–899.

Kater, S. B., Mattson, M. P., Cohan, C., and Connor, J. (1988). Calcium regulation of the neuronal growth cone. *Trends Neurosci.* 11: 315–321.

Kuhn, T. B., Williams, C. V., Dou, P., and Kater, S. B. (1998). Laminin directs growth cone navigation via two temporally and functionally distinct calcium signals. *J. Neurosci.* 18: 184–194.

Lankford, K. L., and Letourneau, P. (1991). Roles of actin filaments and three second messenger systems in short term regulation of chick dorsal root ganglion neurite outgrowth. *Cell Motil. Cytoskel.* 20: 7–29.

LeMasson, G., Marder, E., and Abbott, L. F. (1993). Activity-dependent regulation of conductances in model neurons. *Science* 259: 1915–1917.

Letourneau, P. C., Kater, S. B., and Macagno, E. R. (eds.) (1991). *The Nerve Growth Cone*. New York: Raven Press.

Li, Z., Van Aelst, L., and Cline, H. T. (2000). Rho GTPases regulate distinct aspects of dendritic arbor growth in *Xenopus* central neurons in vivo. *Nature Neurosci.* 3: 217–225.

Lin, C. H., and Forscher, P. (1995). Growth cone advance is inversely proportional to retrograde F-actin flow. *Neuron* 14: 763–771.

Maccioni, R., and Cambiazo, V. (1995). Role of microtubule associated proteins in the control of microtubule assembly. *Physiol. Rev.* 75: 835–864.

Marder, E., Abbott, L. F., Turrigiano, G. G., Liu, Z., and Golowasch, J. (1996). Memory from the dynamics of intrinsic membrane currents. *Proc. Natl. Acad. Aci. U.S.A.* 93: 13481–13486.

Marom, S., and Shahaf, G. (2002). Development, learning and memory in large random networks of cortical neurons: Lessons beyond anatomy. *Quart. Rev. Biophys.* 35: 63–87.

Mattson, M. P. (1988). Neurotransmitters in the regulation of neuronal cytoarchitecture. *Brain Res. Rev.* 13: 179–212.

Mattson, M. P., and Kater, S. B. (1987). Calcium regulation of neurite elongation and growth cone motility. *J. Neurosci.* 7: 4034–4043.

Mattson, M. P., and Kater, S. B. (1989). Excitatory and inhibitory neurotransmitters in the generation and degeneration of hippocampal neuroarchitecture. *Brain Res.* 478: 337–348.

Mattson, M. P., Dou, P., and Kater, S. B. (1988). Outgrowth-regulation actions of glutamate in isolated hippocampal pyramidal neurons. *J. Neurosci.* 8: 2087–2100.

McAllister, A. K. (2000). Cellular and molecular mechanisms of dendrite growth. *Cereb. Cortex* 10: 963–973.

Meinecke, D. L., and Peters, A. (1987). GABA immunoreactive neurons in rat visual cortex. *J. Comp. Neurol.* 261: 388–404.

O'Kusky, J. R. (1985). Synapse elimination in the developing visual cortex: A morphometric analysis in normal and dark-reared cats. *Dev. Brain Res.* 22: 81–91.

Raijmakers, M. E. J., and Molenaar, P. C. M. (1999). A biologically plausible maturation of an ART network. *Lect. Notes Comput. Sci.* 1606: 730–736.

Ramakers, G. J. A., Winter, J., Hoogland, T. M., Lequin, M. B., Van Hulten, P., Van Pelt, J., and Pool, C. W. (1998). Depolarization stimulates lamellipodia formation and axonal but not dendritic branching in cultured rat cerebral cortex neurons. *Dev. Brain Res.* 108: 205–216.

Ramakers, G. J. A., Avci, B., Van Hulten, P., Van Ooyen, A., Van Pelt, J., Pool, C. W., and Lequin, M. B. (2001). The role of calcium signaling in early axonal and dendritic morphogenesis of rat cerebral cortex neurons under non-stimulated growth conditions. *Dev. Brain Res.* 126: 163–172.

Romijn, H. J., Van Marle, J., and Janszen, A. W. J. W. (1993). Permanent increase of the GAD_{67}/synaptophysin ratio in rat cerebral cortex nerve endings as a result of hypoxic ischemic encephalopathy sustained in early postnatal life: A confocal laser scanning microscopic study. *Brain Res.* 630: 315–329.

Romijn, H. J., Voskuyl, R. A., and Coenen, A. M. L. (1994). Hypoxic ischemic encephalopathy sustained in early postnatal life may result in permanent epileptic activity and an altered cortical convulsive threshold in rat. *Epilepsy Res.* 17: 31–42.

Sanes, D. H., and Takács (1993). Activity-dependent refinement of inihibitory connections. *Eur. J. Neurosci.* 5: 570–574.

Sánchez, C., Díaz-Nido, J., and Avila, J. (2000). Phosphorylation of microtubule-associated protein 2 (MAP2) and its relevance for the regulation of the neuronal cytoskeleton function. *Prog. Neurobiol.* 61: 133–168.

Schilling, K., Dickinson, M. H., Connor, J. A., and Morgan, J. I. (1991). Electrical activity in cerebellar cultures determines Purkinje cell dendritic growth patterns. *Neuron* 7: 891–902.

Schilstra, M. J., Bayley, P. M., and Martin, S. R. (1991). The effect of solution composition on microtubule dynamic instability. *Biochem. J.* 277: 839–847.

Shepherd, G. M. (1990). *The Synaptic Organization of the Brain*. Oxford: Oxford University Press.

Stoop, R., and Poo, M. M. (1996). Synaptic modulation by neurotrophic factors: Differential and synergistic effects of brain-derived neurotrophic factor and ciliary neurotrophic factor. *J. Neurosci.* 16: 3256–3264.

Stuart, G. J., and Sakmann, B. (1994). Active propagation of somatic action potentials into neocortical pyramidal cell dendrites. *Nature* 367: 69–72.

Tapon, N., and Hall, A. (1997). Rho, Rac and Cdc42 GTPases regulate the organization of the actin cytoskeleton. *Curr. Opin. Cell Biol.* 9: 86–92.

Torreano, P. J., and Cohan, C. S. (1997). Electrically induced changes in Ca^{2+} in *Helisoma* neurons: Regional and neuron-specific differences and implications for neurite outgrowth. *J. Neurobiol.* 32: 150–162.

Turrigiano, G. G. (1999). Homeostatic plasticity in neuronal networks: The more things change, the more they stay the same. *Trends Neurosci.* 22: 221–227.

Turrigiano, G. G., Abbott, L. F., and Marder, E. (1994). Activity-dependent changes in the intrinsic properties of cultured neurons. *Science* 264: 974–977.

Turrigiano, G. G., Le Masson, G., and Marder, E. (1995). Selective regulation of current densities underlies spontaneous changes in the activity of cultured neurons. *J. Neurosci.* 15: 3640–3652.

Turrigiano, G. G., Leslie, K. R., Desai, N. S., Rutherford, L. C., and Nelson, S. B. (1998). Activity-dependent scaling of quantal amplitude in neocortical neurons. *Nature* 391: 892–896.

Uylings, H. B. M., Van Eden, C. G., Parnavelas, J. G., and Kalsbeek, A. (1990). The prenatal and postnatal development of rat cerebral cortex. In *The Cerebral Cortex of the Rat*, B. Kolb and R. C. Trees, eds. Cambridge, Mass.: MIT Press.

Van Huizen, F., and Romijn, H. J. (1987). Tetrodotoxin enhances initial neurite outgrowth from fetal rat cerebral cortex cells in vitro. *Brain Res.* 408: 271–274.

Van Huizen, F., Romijn, H. J., and Habets, A. M. M. C. (1985). Synaptogenesis in rat cerebral cortex is affected during chronic blockade of spontaneous bioelectric activity by tetrodotoxin. *Dev. Brain Res.* 19: 67–80.

Van Huizen, F., Romijn, H. J., Habets, A. M. M. C., and Van den Hooff, P. (1987a). Accelerated neural network formation in rat cerebral cortex cultures chronically disinhibited with picrotoxin. *Exp. Neurol.* 97: 280–288.

Van Huizen, F., Romijn, H. J., and Corner, M. A. (1987b). Indications for a critical period for synapse elimination in developing rat cerebellar cortex cultures. *Dev. Brain Res.* 13: 1–6.

Van Ooyen, A. (1994). Activity-dependent neural network development. *Network: Comput. Neural Syst.* 5: 401–423.

Van Ooyen, A., and Van Pelt, J. (1994). Activity-dependent outgrowth of neurons and overshoot phenomena in developing neural networks. *J. Theor. Biol.* 167: 27–43.

Van Ooyen, A., and Van Pelt, J. (1996). Complex periodic behaviour in a neural network model with activity-dependent neurite outgrowth. *J. Theor. Biol.* 179: 229–242.

Van Ooyen, A., Van Pelt, J., and Corner, M. A. (1995). Implications of activity-dependent neurite outgrowth for neuronal morphology and network development. *J. Theor. Biol.* 172: 63–82.

Van Ooyen, A., Pakdaman, K., Houweling, A. R., Van Pelt, J., and Vibert, J.-F. (1996). Network connectivity changes through activity-dependent neurite outgrowth. *Neur. Proc. Lett.* 3: 123–130.

Van Oss, C., and Van Ooyen, A. (1997). Effects of inhibition on neural network development through activity-dependent neurite outgrowth. *J. Theor. Biol.* 185: 263–280.

Van Pelt, J., Wolters, P. S., Willems, W. P. A., Rutten, W. L. C., Corner, M. A., Van Hulten, P., and Ramakers, G. J. A. (2003). Developmental changes in firing patterns in neocortical networks in vitro: Longitudinal recordings on multi-electrode arrays. *Exp. Brain Res.*, submitted.

Woolley, C. S. (1999). Structural plasticity of dendrites. In *Dendrites*, G. Stuart, N. Spruston, and M. Häusser, eds. pp. 339–364. Oxford: Oxford University Press.